

Article

Hydrothermally doping valve metal Nb into Titanate nanofibers structure for potentially engineering bone tissue

Yang Tian^{1,2,§}, Parker Cole^{3,§}, Yiting Xiao^{4,§}, Abdussamad Akhter⁵, Trenton Collins⁵, Lu Zhang⁶, Yan Huang^{6,7}, Z. Ryan Tian^{1,2,5,6,*}

¹ Material Science/Engineering, University of Arkansas, Fayetteville, AR 72701, USA

² Institute for Nanoscience/Engineering, University of Arkansas, Fayetteville, AR 72701, USA

³ Biomedical Engineering, University of Arkansas, Fayetteville, AR 72701, USA

⁴ Biological and Agricultural Engineering, University of Arkansas, Fayetteville, AR 72701, USA

⁵ Chemistry and Biochemistry, University of Arkansas, Fayetteville, AR 72701, USA

⁶ Cell/Molecular Biology, University of Arkansas, Fayetteville, AR 72701, USA

⁷ Animal Science, University of Arkansas, Fayetteville, AR 72701, USA

* **Corresponding author:** Z. Ryan Tian, rtian@uark.edu

§ The authors contribute to this work equally.

CITATION

Tian Y, Cole P, Xiao Y, et al.
Hydrothermally doping valve metal Nb into Titanate nanofibers structure for potentially engineering bone tissue. *Nano and Medical Materials*. 2024; 4(1): 375.
<https://doi.org/10.59400/nmm.v4i1.375>

ARTICLE INFO

Received: 30 December 2023

Accepted: 26 February 2024

Available online: 7 March 2024

COPYRIGHT



Copyright © 2024 by author(s).
Nano and Medical Materials is published by Academic Publishing Pte. Ltd. This work is licensed under the Creative Commons Attribution (CC BY) license.
<https://creativecommons.org/licenses/by/4.0/>

Abstract: Recent research efforts in bone tissue engineering have been primarily directed towards manufacture-viable synthesis of biomaterials that can significantly enhance the biocompatibilities and osteogenic capabilities on the new biomaterials. This paper presents a straightforward, cost-effective, optimized, and well-controlled hydrothermal synthesis of Nb-doped potassium titanate nanofibers in high-purity. Characterization data revealed that the Nb-doping potassium titanate maintained the crystal structure, showing great promise for applications in bone tissue engineering.

Keywords: nanosynthesis; titanate nanofiber; bone tissue engineering; bone scaffold; niobium dopant; pro-bone elements

1. Introduction

Nanomaterials possess the capability to bolster mechanical properties, release therapeutic ions or molecules into the adjacent environment to boost osteoblast cell recruitment, adhesion, growth, and differentiation; improve surface energy and protein adsorption, affect integrin binding; and function as a radiopacifier for improved visualization in X-ray imaging [1–6]. With the advent of nanotechnology, tissue engineering has advanced significantly, encompassing improvements ranging from architectural design and stability to multifunctional materials.

Given that bone is inherently a bio-nanocomposite, our objective has been to develop nanoscale substitutes of natural bone by utilizing novel materials that could promote bone tissue growth for bone regeneration. Recent studies have provided new insights into the mechanisms underlying the crucial role of nanotechnologies in orthopedic applications. Nanoscale characteristics such as grain size, pore dimensions and configuration, surface texture, surface-to-volume ratio, surface hydrophilicity, and related energetics are recognized as key contributors to such enhanced performance in bone tissue regeneration and integration [7]. To this end, a continuously expanding range of nanomaterials and nanotechnologies has been developed, examined, and applied within the field of bone tissue engineering [8–10].

Titanium dioxide has attracted growing interest with the merging of orthopedics and nanomaterial science. This is largely attributed to the well-established fact that Ti metal surfaces oxidize when in contact with air, forming a dense layer of native titanium dioxide (TiO₂) on the surface. Studies have revealed that anodization, a process to uniformly create an oxide surface coating, fosters the formation of a surface layer that is biologically compatible and promotes osteogenesis. Advancements facilitated by nanomaterial chemistry have significantly advanced this field of study, with numerous laboratories achieving structural control over the TiO₂ layer in morphologies like nanofibers and nanotubes [11,12]. Remarkably, it has also been found that certain synthetic methods can lead to the formation of an ionic intermediate titanate structure. This layered clay-like crystalline structure, made up of edge-sharing TiO₆ octahedra intercalated with cations, has been recognized for its ability to facilitate hydroxyapatite formation in simulated body fluid (SBF) [13]. In a hydrothermal environment with an aqueous sodium (or potassium) hydroxide solution, powdery TiO₂ minerals, such as rutile and anatase, were involved in the chemical reaction to form either Na- or K-titanate nanotubes or nanowires, with the specific morphology significantly affected by the thermal conditions of the reaction. Thus-formed ionic layered structure acts as a cation “reservoir”, allowing for potential ion exchange with cations in body fluids. This enables an autonomous, real-time balancing of cations in situ, aiding in the growth of bone tissue. Na/K-titanate is in a hypotonic state compared to the concentration of calcium (Ca²⁺) in the SBF inducing the ion exchange of Na⁺ or K⁺ ions with Ca²⁺. Subsequently, phosphate anions in the body fluid, including (PO₃)³⁻, (HPO₃)²⁻, and (H₂PO₃)⁻, interact with the Ca²⁺ on the titanate surface. This interaction leads to the formation of hydrated calcium phosphate, known as hydroxyapatite, a critical component of natural bone essential for creating an osteogenic/osteoconductive environment [13].

In addition, the nanomaterials with pro-bone elements like Zirconium (Zr), Niobium (Nb), or Tantalum (Ta) have been demonstrated to enhance the performance of osteointegration [14–17]. However, the practical implementation of these pro-bone element oxides has been hurdled by the often-elevated costs and synthesis complexities. Therefore, doping titanate nanofibers with pro-bone elements emerges as an advantageous alternative approach to create novel bone implant materials. In this work, we systematically conducted nanosynthesis to produce long and pristine Nb-doped titanate nanofibers with strong market feasibility for orthopedic implants. The optimization of doping was verified through the analysis of characterization data obtained from scanning electron microscopy with an energy-dispersive elemental analyzer (SEM-EDX) and X-ray diffraction (XRD).

2. Materials and methods

2.1. Nanofiber synthesis

The Nb-doped potassium titanate nanofibers were prepared following a published protocol [18–21] with some modifications. Briefly, in a Teflon cup containing 50 mL water solution of 10 M KOH, 500 mg of TiO₂ powder (Aeroxide P25) was added to the Teflon and stirred for about 5 min with a Teflon-coated

magnetic stirring bar on an electrical stirrer. Thereafter, Niobium oxide powder (chemical grade, from Alfa Aesar) was mixed with the KOH solution to form a mixture upon stirring. Here, the molar ratio of Nb-dopant to Titanate was widely varied from 1%–4%.

Next, the mixture containing Teflon cup was sealed in an autoclave container, heated in an oven at 240 °C for 72 hours and then cooled down in air. The white powdery product was collected, water-washed until pH = 7, and finally air-dried for the characterizations. To keep the nanofiber lattice intact, it is important to do the water-washing step carefully, as detailed separately below.

2.2. Post synthesis washing

The fibers were formed as a slurry from the high alkalinity environment in the autoclave treatment. To remove the residual KOH, the white slurry went through a well-controlled neutralization process. The nanofiber slurry was first centrifuged for 5 min at 4000 rpm. The supernatant was decanted and then mixed with deionized water to form another slurry with a lower KOH content, which was repeated until the supernatant's pH = 7.

2.3. Characterization

The SEM-EDX analysis was carried out on the FEI Nova NanoLab 200 to assess nanofiber morphology and chemical composition. Typically, the fiber sample was placed on an aluminum holder to let the sample dry in air. Once dried, the holder was placed in a plasma sputtering coater with an Au target to coat the sample surface with Au. The XRD was performed with the Rigaku MiniFlex II Desktop X-ray diffractometer using monochromatized Cu-K α ($\lambda = 1.5406 \text{ \AA}$) at 30 kV and 15 mA, in the range of 2θ from 5° to 60° at a speed of 1°/min. to assess crystal structure.

3. Results and discussion

Niobium doping

The Nb-doped potassium titanate nanofibers underwent self-assembly, forming a bone-mimetic bio-scaffold structure upon desiccation as illustrated in **Figure 1**. These self-assembled nanowires created porous structures, facilitating effective bone tissue adhesion to the bio-scaffold. Moreover, the increased surface area provided by these structures enhances osteoblast cell adhesion.

At higher magnification (**Figure 2a**), the clean and well-crystallized long nanofibers in self-entangled sheets can be clearly seen, which is a characteristic of the Nb-doped potassium titanate nanofibers. The nanofiber length extends into the microns range whereas the width of these fibers is under 100 nm. Additionally, **Figure 2a** shows the relatively smooth surface of the high length to width ratio (or aspect ratio) nanofibers, suggesting an optimal control over the nanosynthesis parameters to achieve the uniformly distributed Ta-doping throughout the lattice.

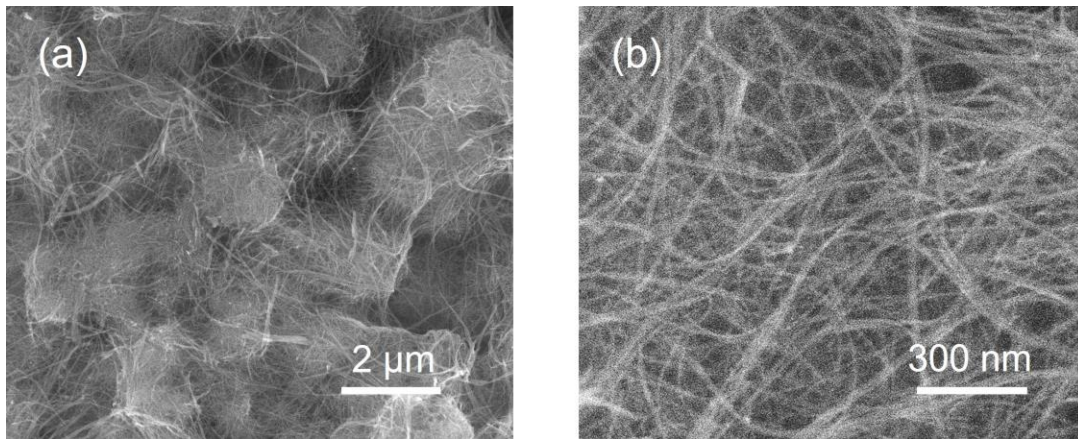


Figure 1. SEM Micrographs of Nb-doped potassium titanate.

On the EDX map, the Nb dopants (**Figure 2d**) are distributed on the fibers showing overlap with the Ti species (**Figure 2b**), indicating the lattice building blocks of the smaller $[\text{TiO}_6]$ octahedra more than the larger $[\text{NbO}_6]$ octahedra. Seemingly, the $[\text{NbO}_6]$ octahedra are well-dispersed allowing for the structural distortion of each $[\text{NbO}_6]$ octahedron to not destroy the lattice structural continuity. The high dispersion of Nb dopant in the nanofiber structure suggests the optimal doping conditions that support **Figure 1**.

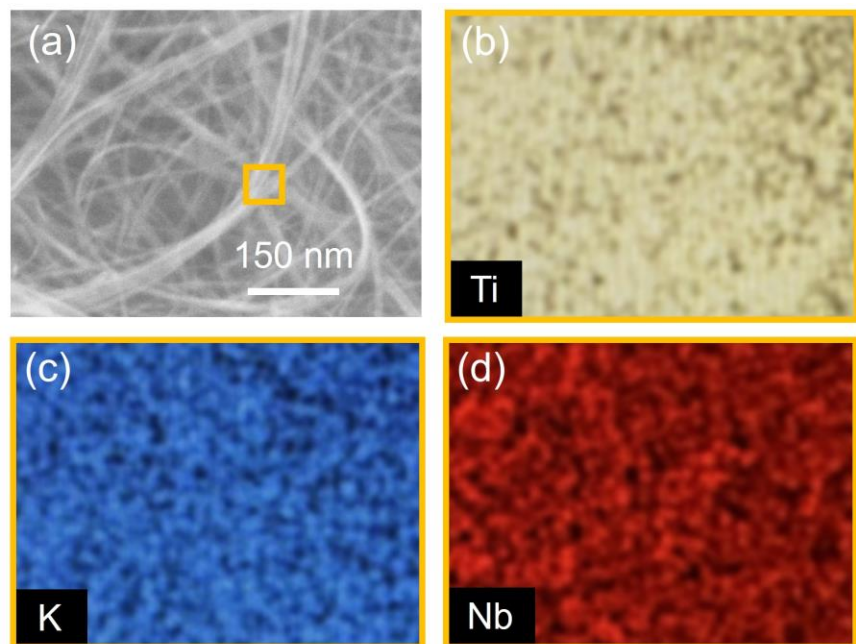


Figure 1. Element Dispersive EDX Mapping of the Nb-Doped Potassium Titanate Nanofibers. (a) the high-resolution SEM of Nb-doped potassium with the yellow box for EDX mapping; The EDX mapping showed (b) K; (c) Ti; and (d) Nb are evenly distributed on the titanate nanofibers.

The nanofiber crystal structure can be characterized using the XRD patterns (**Figure 3**). All the XRD peaks of (200), (110), (310), $(31\bar{2})$, $(40\bar{4})$, and (020) can be assigned to the layered $\text{K}_2\text{Ti}_6\text{O}_{13}$ titanate lattice (JCPDS No. 40-0403). No residual impurity was detected, as evidenced by no extra peaks in the XRD pattern due to the

XRD detection limit, which indicates that the larger $[\text{NbO}_6]$ octahedron is well doped in the titanate crystal structure to maintain the lattice integrity and nanofiber structure.

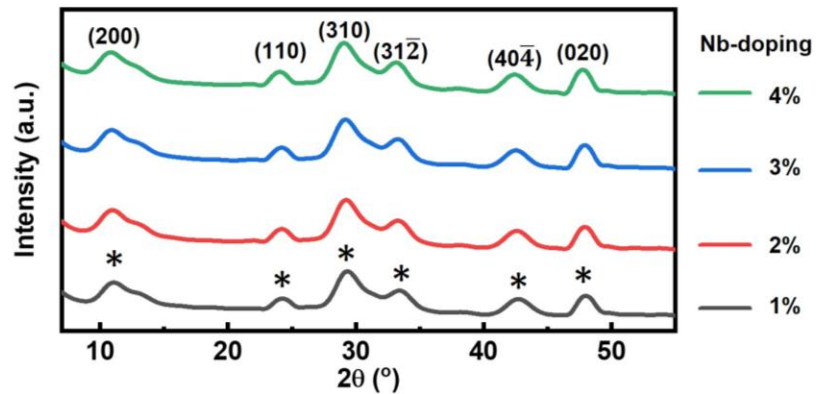


Figure 2. X-Ray diffraction of Nb-doped potassium titanate nanofibers with variant doping percentage.

Comparing the XRD patterns with and without doping (**Figure 4a**), the large Nb-dopant increases the d-space between adjacent titanate sheets by shifting the XRD peak to $d_{(200)} = 8.18147 \text{ \AA}$ (or a lower 2-theta angle at $2\theta = 10.81^\circ$) [20,22]. This is in contrast with the undoped nanofiber's smaller d-space of $d_{(200)} = 7.7415 \text{ \AA}$ at a higher 2-theta angle ($2\theta = 11.43^\circ$). This interlayer spacing expansion is indicative of Nb substitutional doping within the titanate lattice. More specifically, the ionic radius of Nb^{5+} (64 pm) is larger than that of Ti^{4+} (53 pm) which leads to Nb^{5+} species replacing Ti^{4+} within the titanate lattice. Substitutional doping of larger ions within the native lattice increases lattice parameters and cell volume resulting in shifts to lower diffraction angles [23]. Moreover, the doped samples XRD patterns show no structural impurity. This is because all the XRD peaks are in the same width and can be indexed to that of potassium titanate, as others including those reported in literature by our lab [18–20].

Evidently, within the K-titanate nanofiber's clay-like layered crystal structure, the Ti^{4+} -based $[\text{TiO}_6]$ octahedra have undergone partial substitution by the Nb^{5+} -based $[\text{NbO}_6]$ octahedra, confirming the intentional doping of Nb^{5+} . From a steric perspective, the larger $[\text{NbO}_6]$ compared to $[\text{TiO}_6]$ would naturally position itself on the nanofiber surface to reduce perturbations in the predominantly $[\text{TiO}_6]$ crystal lattice. Such surface-exposed $[\text{NbO}_6]$ units have been recognized to facilitate bone-tissue adhesion, as corroborated by previous studies [1,14,24]. Additionally, the proximal interlayer K^+ cations to the $[\text{NbO}_6]$ in the K-titanate nanofiber are predisposed to be swiftly substituted by Ca^{2+} cations from body fluids. This accelerates the formation of hydrated calcium phosphates, or hydroxyapatite, on the nanofiber, consistent with findings from other research groups using SBF [13,25]. The robust interaction between the hydroxyapatite layer and the underlying titanate nanofiber ensures sustained bone tissue adhesion on the hydroxyapatite-supported nanofiber, crafting an optimal osteogenic/osteoconductive milieu [13]. Therefore, the refined surface characteristics of titanate nanofibers present a complementary approach to existing methodologies, enhancing the osteoconductivity of bone-

scaffolds [14,24,26]. Fundamentally, this research introduces a pioneering and economically viable technique for incorporating Nb (V) into the titanate nanofiber matrix, marking a significant stride in the realm of orthopedic nanomedicine.

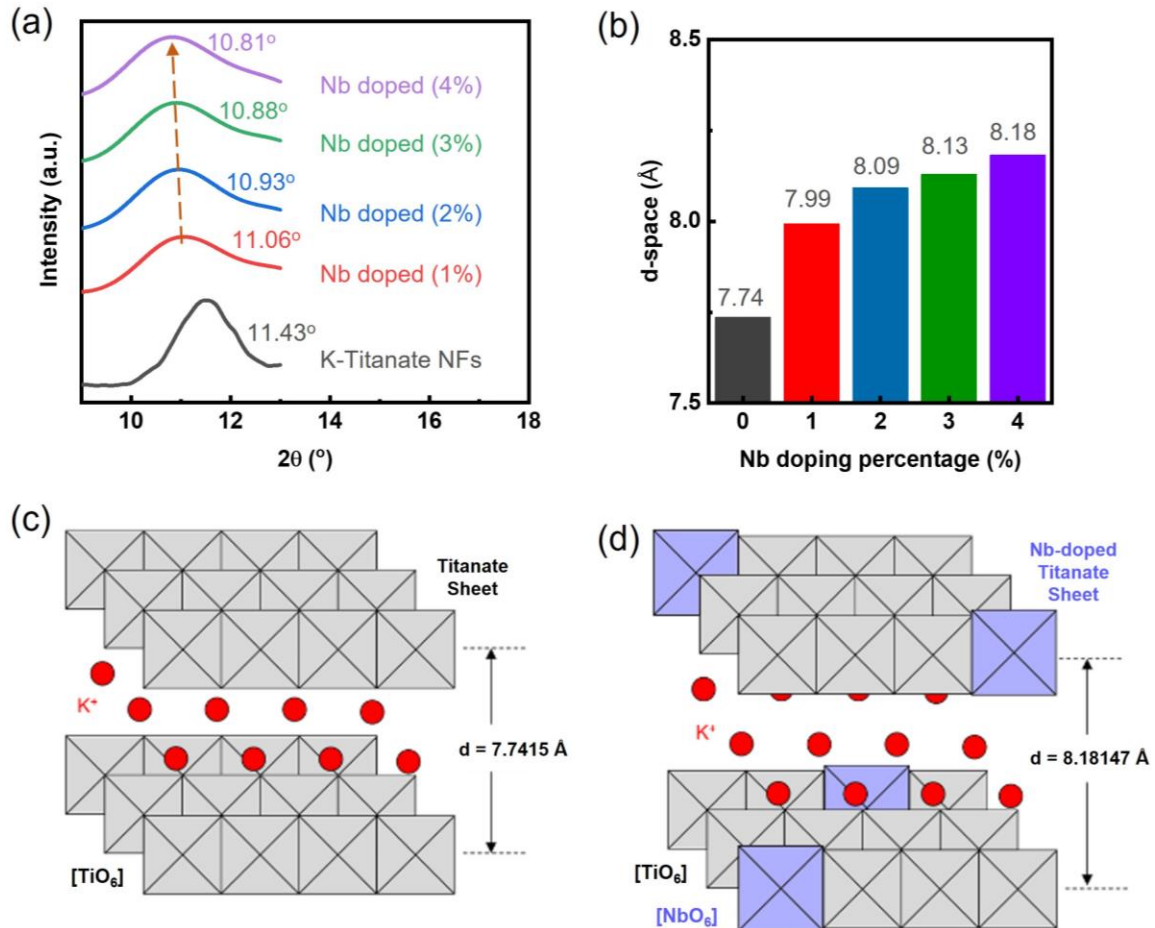


Figure 3. (a) XRD analysis of Nb-doped potassium titanate nanofibers; with (b) d-space; (c) Titanate Sheet; and (d) Nb-dopant impact on the titanate crystal structure.

4. Conclusions

Niobium-doped potassium titanate nanofibers have been successfully produced using a simple hydrothermal method. This approach is notably innovative, particularly in the field of orthopedic nanomedicine, as far as we are aware. After doping, the nanofibers maintained their morphology, chemical composition, and crystallinity, suggesting that the hydrothermal method used for doping the crystal framework is effective. Moreover, the dopant concentrations were carefully controlled to ensure no negative impact on the nanofiber's lattice structure. This is crucial for preserving their desired properties for the intended uses.

Author contributions: Investigation, YT, YX, AA and TC; writing—original draft preparation, YT and ZRT; writing—review and editing, YT, PC, LZ, YH and ZRT. All authors have read and agreed to the published version of the manuscript.

Acknowledgments: The team would like to thank Paula Prescott and Connie Dixon for ordering lab supplies and managing financial reimbursement. The team also

would like to thank Kz Shein, Zay Lynn, and David N. Parette for the technical support.

Data availability statement: Applicable for reasonable request.

Conflict of interest: The authors declare no conflict of interest.

References

1. Zhang B, Li J, He L, et al. Bio-surface coated titanium scaffolds with cancellous bone-like biomimetic structure for enhanced bone tissue regeneration. *Acta Biomaterialia*. 2020; 114: 431-448. doi: 10.1016/j.actbio.2020.07.024
2. Min Q, Liu J, Zhang Y, et al. Dual Network Hydrogels Incorporated with Bone Morphogenic Protein-7-Loaded Hyaluronic Acid Complex Nanoparticles for Inducing Chondrogenic Differentiation of Synovium-Derived Mesenchymal Stem Cells. *Pharmaceutics*. 2020; 12(7): 613. doi: 10.3390/pharmaceutics12070613
3. Wu T, Li B, Wang W, et al. Strontium-substituted hydroxyapatite grown on graphene oxide nanosheet-reinforced chitosan scaffold to promote bone regeneration. *Biomaterials Science*. 2020; 8(16): 4603-4615. doi: 10.1039/d0bm00523a
4. Oudadesse H, Najem S, Mosbahi S, et al. Development of hybrid scaffold: Bioactive glass nanoparticles/chitosan for tissue engineering applications. *Journal of Biomedical Materials Research Part A*. 2020; 109(5): 590-599. doi: 10.1002/jbm.a.37043
5. Nie L, Deng Y, Li P, et al. Hydroxyethyl Chitosan-Reinforced Polyvinyl Alcohol/Biphasic Calcium Phosphate Hydrogels for Bone Regeneration. *ACS Omega*. 2020; 5(19): 10948-10957. doi: 10.1021/acsomega.0c00727
6. Photo-crosslinked alginate nano-hydroxyapatite paste for bone tissue engineering - IOPscience. Available online: <https://iopscience.iop.org/article/10.1088/1748-605X/ab9551/meta> (accessed on 14 November 2023).
7. Yang L, Gao C, Wei D, et al. Nanotechnology for treating osteoporotic vertebral fractures. *International Journal of Nanomedicine*. 2015; 5139. doi: 10.2147/ijn.s85037
8. Venkataramana C, Botsa SM, Shyamala P, et al. Photocatalytic degradation of polyethylene plastics by NiAl₂O₄ spinels - synthesis and characterization. *Chemosphere*. 2021; 265: 129021. doi: 10.1016/j.chemosphere.2020.129021
9. Saravanan S, Vimalraj S, Anuradha D. Chitosan based thermoresponsive hydrogel containing graphene oxide for bone tissue repair. *Biomedicine & Pharmacotherapy*. 2018; 107: 908-917. doi: 10.1016/j.biopha.2018.08.072
10. Mohammadi M, Mousavi Shaegh SA, Alibolandi M, et al. Micro and nanotechnologies for bone regeneration: Recent advances and emerging designs. *Journal of Controlled Release*. 2018; 274: 35-55. doi: 10.1016/j.jconrel.2018.01.032
11. Aldaadaa A, Al Qaysi M, Georgiou G, et al. Physical properties and biocompatibility effects of doping SiO₂ and TiO₂ into phosphate-based glass for bone tissue engineering. *Journal of Biomaterials Applications*. 2018; 33(2): 271-280. doi: 10.1177/0885328218788832
12. Hashemi A, Ezati M, Mohammadnejad J, et al. Chitosan Coating of TiO₂ Nanotube Arrays for Improved Metformin Release and Osteoblast Differentiation. *International Journal of Nanomedicine*. 2020; 15: 4471-4481. doi: 10.2147/ijn.s248927
13. Liang F, Zhou L, Wang K. Apatite Formation on Porous Titanium by Alkali and Heat-Treatment. *Surface and Coatings Technology*. 2003; 165(2): 133-139. doi: 10.1016/S0257-8972(02)00735-1
14. Marins NH, Lee BEJ, e Silva RM, et al. Niobium pentoxide and hydroxyapatite particle loaded electrospun polycaprolactone/gelatin membranes for bone tissue engineering. *Colloids and Surfaces B: Biointerfaces*. 2019; 182: 110386. doi: 10.1016/j.colsurfb.2019.110386
15. Cadafalch Gazquez G, Chen H, Veldhuis SA, et al. Flexible Yttrium-Stabilized Zirconia Nanofibers Offer Bioactive Cues for Osteogenic Differentiation of Human Mesenchymal Stromal Cells. *ACS Nano*. 2016; 10(6): 5789-5799. doi: 10.1021/acsnano.5b08005
16. Hwang C, Park S, Kang IG, et al. Tantalum-coated polylactic acid fibrous membranes for guided bone regeneration. *Materials Science and Engineering: C*. 2020; 115: 111112. doi: 10.1016/j.msec.2020.111112
17. Zhang J, Huang D, Liu S, et al. Zirconia toughened hydroxyapatite biocomposite formed by a DLP 3D printing process for potential bone tissue engineering. *Materials Science and Engineering: C*. 2019; 105: 110054. doi: 10.1016/j.msec.2019.110054
18. Dong W, Cogbill A, Zhang T, et al. Multifunctional, Catalytic Nanowire Membranes and the Membrane-Based 3D Devices. *The Journal of Physical Chemistry B*. 2006; 110(34): 16819-16822. doi: 10.1021/jp0637633

19. Dong W, Zhang T, Epstein J, et al. Multifunctional Nanowire Bioscaffolds on Titanium. *Chemistry of Materials*. 2007; 19(18): 4454-4459. doi: 10.1021/cm070845a
20. Cole P, Tian Y, Thornburgh S, et al. Hydrothermal synthesis of valve metal Zr-doped titanate nanofibers for bone tissue engineering. *Nano and Medical Materials*. 2023; 3(2): 249. doi: 10.59400/nmm.v3i2.249
21. Xiao Y, Tian Y, Zhan Y, Zhu J. Degradation of organic pollutants in flocculated liquid digestate using photocatalytic titanate nanofibers: Mechanism and response surface optimization. *Frontiers of Agricultural Science and Engineering*. 2023; 10(3), 492-502. doi: 10.15302/j-fase-2023503
22. Yuan ZY, Zhang XB, Su BL. Moderate hydrothermal synthesis of potassium titanate nanowires. *Applied Physics A*. 2004; 78(7): 1063-1066. doi: 10.1007/s00339-003-2165-x
23. Bi H, Zhu S, Liang Y, et al. Nb-Doped TiO₂ with Outstanding Na/Mg-Ion Battery Performance. *ACS Omega*. 2023; 8(6): 5893-5900. doi: 10.1021/acsomega.2c07689
24. Balbinot G de S, Bahlis EA da C, Visioli F, et al. Polybutylene-adipate-terephthalate and niobium-containing bioactive glasses composites: Development of barrier membranes with adjusted properties for guided bone regeneration. *Materials Science and Engineering: C*. 2021; 125: 112115. doi: 10.1016/j.msec.2021.112115
25. Wang X, Liu SJ, Qi YM, et al. Behavior of potassium titanate whisker in simulated body fluid. *Materials Letters*. 2014; 135: 139-142. doi: 10.1016/j.matlet.2014.07.145
26. Capanema N, Mansur A, Carvalho S, et al. Niobium-Doped Hydroxyapatite Bioceramics: Synthesis, Characterization and In Vitro Cytocompatibility. *Materials*. 2015; 8(7): 4191-4209. doi: 10.3390/ma8074191